INSTITUTE OF PHYSICS PUBLISHING JOURNAL OF PHYSICS B: ATOMIC, MOLECULAR AND OPTICAL PHYSICS

J. Phys. B: At. Mol. Opt. Phys. **34** (2001) L203–L210 www.iop.org/Journals/jb PII: S0953-4075(01)19609-4

LETTER TO THE EDITOR

The helium trimer has no bound rotational excited states

T G Lee, B D Esry, Bing-Cong Gou[1] and C D Lin

Department of Physics, Cardwell Hall, Kansas State University, Manhattan, KS 66506, USA

Received 29 November 2000, in final form 14 February 2001

Abstract

We have searched for bound states of helium trimers with nonzero angular momenta. Including only pair interactions between helium atoms, we solved the Schrödinger equation in hyperspherical coordinates in the adiabatic approximation. From the resulting potential curves—which are mostly repulsive for nonzero angular momenta—we conclude that there are no bound rotational excited states in any of the isotopes of the helium trimer. The symmetry properties of the trimer wavefunctions in the body-fixed frame are also analysed.

In recent years the properties of very weakly bound small ^{4}He clusters have been examined in a variety of studies, both theoretical [1–6] and experimental [7–10]. To set the energy scale for these systems, the ^{4}He dimer is bound by only about 1.3 mK. For the $^4He_3$ trimer, extensive calculations [1] have shown that there are two bound states with binding energies of about 105 and 0.808 mK. The excited state has been shown [1, 3] to have properties characteristic of an Efimov state where the binding energy is exponentially small and the size is exponentially large with respect to a two-body potential parameter such as the scattering length. Practically all the calculations that have been carried out for helium trimers have dealt with states of zero total angular momentum, $J = 0$. Since there are two bound states for $J = 0$, it has been speculated [6] that there may exist bound states for nonzero angular momenta and that these states may exhibit properties of Efimov states as well. In fact, based on the rigid-rotor model, an estimate of the rotational energy using parameters from the $^4He_3$ ground state suggests that a state with one unit of angular momentum is close to being bound. Such a simple estimate, however, can be grossly in error since quantum statistics are not accounted for in such a perturbative estimate. The behaviour of few-body quantum systems is actually severely constrained by the symmetries imposed by quantum statistics [11].

In this letter we report the results of a search for the bound states of helium trimers with nonzero angular momenta. Both $^4He_3$ and $^4He_2{}^3$He are examined to investigate the effect of quantum statistics on the calculated energies. We conclude that in both systems there are no

[1] Permanent address: Department of Applied Physics, Beijing Institute of Technology, Beijing 100081, People's Republic of China.

0953-4075/01/070203+08$30.00

bound states for nonzero angular momenta. Thus, the only bound states for $^4He_3$ are the two $J = 0$ states, and the only bound state for $^4He_2{}^3He$ is the $J = 0$ ground state.

The calculations were performed using hyperspherical coordinates. Let $\vec{\rho}_1$ be the vector connecting particle 1 to 2, and $\vec{\rho}_2$ the vector from the centre of mass of 1 and 2 to particle 3. For $^4He_2{}^3He$, the two identical particles are designated as 1 and 2. The mass-weighted hyperspherical coordinates are defined by

$$\mu R^2 = \mu_1 \rho_1^2 + \mu_2 \rho_2^2$$
$$\tan\phi = \sqrt{\frac{\mu_2}{\mu_1}} \frac{\rho_2}{\rho_1}.$$

We further define the angle between $\vec{\rho}_1$ and $\vec{\rho}_2$ to be θ. In the equation above, μ_1 is the reduced mass of particles 1 and 2, and μ_2 is the reduced mass of particles (1 + 2) and 3. In this letter we choose the scaling factor $\mu = \sqrt{\mu_1 \mu_2}$; the mass of ^4He is 7296.2994 au, and the mass of ^3He is 5497.8852 au. Atomic units are used unless otherwise specified.

We solve the Schrödinger equation in the adiabatic representation

$$\psi(R, \phi, \theta, \omega) = \sum_\nu F_\nu(R) \Phi_\nu(R; \phi, \theta, \omega),$$

where ω is the set of Euler angles that defines the body frame with respect to the laboratory-fixed frame. We choose the body-frame z'-axis to be along $\vec{\rho}_1$, and the y'-axis to be perpendicular to the plane of the three particles. The x'-axis lies in the plane such that (x', y', z') forms an orthogonal set of axes. In the adiabatic approach, R is treated as a fixed parameter, and the adiabatic potential curves are obtained by solving

$$\left(\frac{\Lambda^2 - \frac{1}{4}}{2\mu R^2} + V \right) \Phi_\nu(R; \phi, \theta, \omega) = U_\nu(R) \Phi_\nu(R; \phi, \theta, \omega). \tag{1}$$

The explicit form of the grand angular momentum operator Λ^2 is given elsewhere [12], and $V = V_{12} + V_{23} + V_{31}$ where V_{ij} is the pair interaction between particles i and j, taken from Aziz and Slaman [13] (in their paper, this potential is designated LM2M2 with add-on). For a state with angular momentum J and parity π, we expand the channel function as

$$\Phi_\nu^{JM\pi}(R; \phi, \theta, \omega) = \sum_I \bar{D}_{IM}^{J\pi}(\omega) \psi_{I\nu}(R; \theta, \phi)$$

where $I\,(M)$ is the projection of J on the body-fixed (laboratory-fixed) quantization axis and $\bar{D}_{IM}^{J\pi}(\omega)$ is the symmetrized D-function. In the following we will call $\psi_{I\nu}(R; \theta, \phi)$ the Ith rotational component wavefunction. This expansion allows equation (1) to be reduced to a set of coupled equations in the two variables (ϕ, θ), which we solve using the B-spline method.

In figure 1 we show the potential curves for $^4He_3$ obtained for $(J^\pi) = (0^+, 1^+, 1^-, 2^+, 2^-, 3^+, 3^-)$. For 0^+, the potential curve is identical to the one obtained by Esry *et al* [1]. By solving the hyper-radial equation with this potential (but including the diagonal correction term $-\frac{1}{2\mu}\langle \Phi_\nu(R) | \mathrm{d}^2/\mathrm{d}R^2 | \Phi_\nu(R) \rangle$), two 0^+ bound states were obtained by Esry *et al* [1] at -105 and -0.808 mK with respect to the dimer threshold, in general agreement with other calculations. From figure 1 we note that the potential curves for other values of J^π are all repulsive. Such repulsive curves do not support any bound states. Based upon these curves, we can conclude that there are no bound states for $^4He_3$ trimers with nonzero angular momentum. Although the calculations were carried out using the pair interaction of Aziz and Slaman [13], the adiabatic hyperspherical potential curves are changed only slightly when other helium pair interactions are used, as demonstrated by Esry *et al* [1] for $J = 0$. Thus, the conclusion that no bound states exist for nonzero angular momenta is not expected to change for calculations using other accurate helium interaction potentials. It should be noted that the pair potential

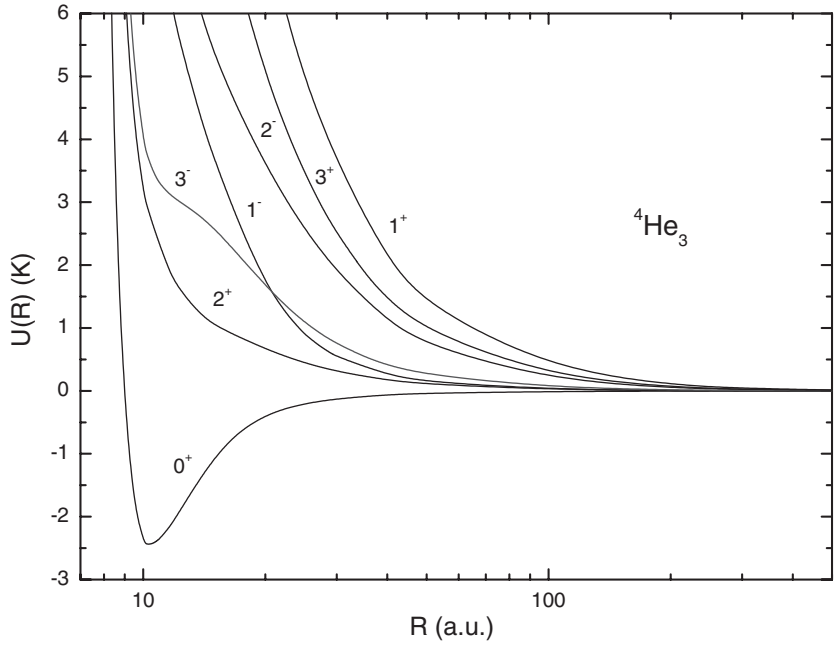

Figure 1. Lowest adiabatic hyperspherical potential curves for $^4He_3$, for each J^π symmetry indicated.

does not include the retardation effect. This effect, however, is estimated [6] to *decrease* the binding and hence does not change our conclusion.

Bound states for $^4He_3$ have been sought by Bruch [6] for the 1^- and 2^+ symmetries. He used totally symmetric variational trial functions for each symmetry and obtained upper bounds that lie above the $^4He_2$ threshold. Since the variational wavefunction used was limited, he concluded that rotational states, if they exist, would have binding energies of less than 1 mK. We note that he found the energy ordering of the 1^- and 2^+ states to be opposite to that shown in figure 1, possibly also due to the limitations of the trial wavefunctions. The 1^- symmetry has also been studied by Nielsen [15] using the coordinate space Faddeev approach coupled with an adiabatic hyperspherical approximation. For 1^-, he also found a completely repulsive potential for $^4He_3$. Based on our adiabatic potential curves for several symmetries, our conclusion is more definite. The curves in figure 1 have no attractive wells and so do not support any bound states for $J \neq 0$.

In figure 2 we show the potential curves for $^4He_2{}^3He$. It is interesting to note that the order of the J^π curves differs from that shown in figure 1 for $^4He_3$: in particular, the 1^- curve is the second lowest state for $^4He_2{}^3He$. This is the result of quantum statistics: the wavefunction for $^4He_3$ must be symmetric under exchange of any pair of particles; for $^4He_2{}^3He$, the wavefunction needs to be symmetric only under the exchange of the two ^4He atoms. We explore the consequences of the different permutational symmetry requirements further below.

In the present calculation, the permutational symmetry is not imposed directly in the numerical solution of equation (1) primarily because it is not a simple matter to impose this symmetry *a priori* in the Delves coordinates. Such a procedure is more easily carried out in Smith–Whitten-type coordinates [14]. Instead, the permutation symmetry is identified in the calculated solutions. To illustrate this point, figure 3 shows the potential curves calculated for

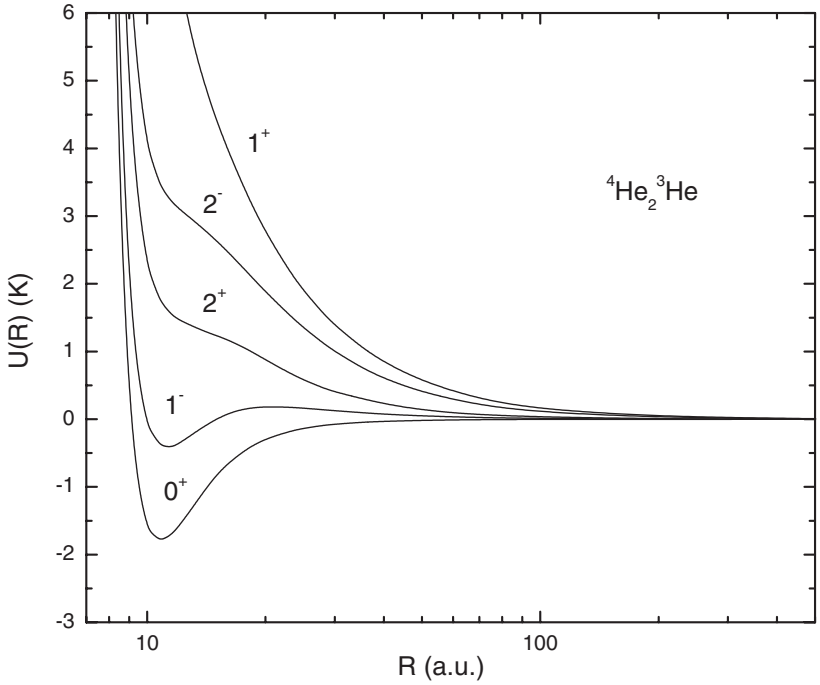

Figure 2. Lowest adiabatic hyperspherical potential curves for $^4He_2{}^3He$, for each J^π symmetry indicated.

1^- without imposing the fact that $^4He_3$ is a bosonic system. The eigensolutions consist of wavefunctions that are totally symmetric, totally antisymmetric, and also of mixed symmetry. The symmetric solution is, of course, the physical one for the three-boson $^4He_3$. The other three are relevant for atoms with nonzero spins. The mixed-symmetry states have to be coupled to spin functions to yield total wavefunctions of the appropriate symmetry. The mixed-symmetry states can be easily identified since their energies are doubly degenerate. Among the four curves in figure 3, the mixed-symmetry curves are indicated by dotted lines. The totally symmetric curve is denoted by a solid curve, and the totally antisymmetric curve is denoted by a dashed curve. We note that the von Neumann–Wigner non-crossing rule from molecular structure applies here so that curves of different symmetry can cross.

We can most easily differentiate the totally symmetric state from the totally antisymmetric state by examining the wavefunction with respect to the interchange of particles 1 and 2. Under this interchange, the components of the channel function should simply be symmetric or antisymmetric about $\theta = \pi/2$. With our choice of quantization axis, an interchange of particles 1 and 2 gives a phase $P(-1)^{J-I}$ from the $\bar{D}$ function [16], where P is the reflection symmetry with respect to the plane of the three particles; $P = +1$ if $\pi = (-1)^J$ and $P = -1$ if $\pi = -(-1)^J$. Since the total wavefunction must be symmetric with respect to the exchange of particles 1 and 2, the symmetry condition for each I-component, $\psi_{I\nu}(R; \theta, \phi)$, is also given by $P(-1)^{J-I}$. For 1^- states, for example, the $I = 0(1)$ component must be antisymmetric (symmetric) with respect to $\theta = \pi/2$. This procedure is sufficient to allow us to identify the curve with the correct symmetry. In figure 3 the correct curve for the bosonic $^4He_3$ is drawn as a solid line. It is *not* the lowest curve. (The higher-lying curves of figure 3 were not analysed since they are irrelevant for the present purpose.)

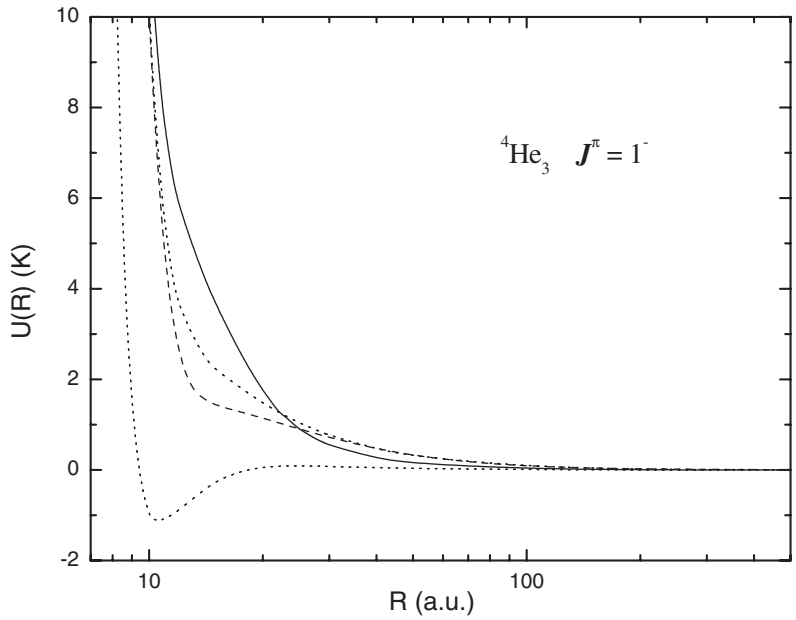

Figure 3. Hyperspherical potential curves for $^4He_3$ without imposing any permutational symmetry. The curve with the correct boson statistics is indicated by the solid curve. The totally antisymmetric solution is shown with a dashed curve, and the mixed-symmetry solutions are shown with dotted curves. Only the curves shown were analysed.

For $^4He_2{}^3He$, the curves are quite close to the curves in figure 3 for which the symmetry condition is not imposed. However, each pair of degenerate curves now splits into two distinct curves. The correct curve for $^4He_2{}^3He$ is the lowest one for which the wavefunction is symmetric under the exchange of particles 1 and 2. The procedure described in the last paragraph can be used to identify this curve. In this case, the correct curve is the lowest curve. Consideration of quantum statistics thus explains why the 1^- curve for $^4He_2{}^3He$, shown in figure 2, is much lower than the 1^- curve in $^4He_3$, shown in figure 1. Note that the 1^- curve for $^4He_2{}^3He$ has a small well. Direct solution of the hyper-radial equation for this potential shows that this well is too shallow to support a bound state since the energy thus obtained is a rigorous lower bound to the exact ground state energy [17]. Further, our calculations show that the dimer potential must be made more than 20% deeper before this well will support a bound state. Neither of the major inaccuracies in the interaction potential used—neglect of three-body effects and inexact two-body potentials—can account for a change of this magnitude. These inaccuracies are expected to be on the order of one per cent or less [18, 19].

It is interesting to ask why the $^4He_3$ potential curves for different values of J^π appear in the order shown in figure 1. We emphasize that this is the result of quantum statistics. The effect of boson statistics from exchanging particles 1 and 2 on the rotational component wavefunction $\psi_{Iv}(R; \theta, \phi)$ has been addressed in the last two paragraphs, but the effects of interchanging 1 and 3 or 2 and 3 have not yet been addressed. In fact, the body-frame quantization axis chosen in our calculation is not the most convenient for addressing the symmetry of three identical particles. A better quantization axis turns out to be one perpendicular to the plane of the three particles. Using this quantization axis, Bao *et al* [11] analysed the symmetry properties of each rotational component wavefunction. They showed that quantum symmetry often imposes nodal surfaces on the rotational component wavefunctions. Since each nodal surface implies

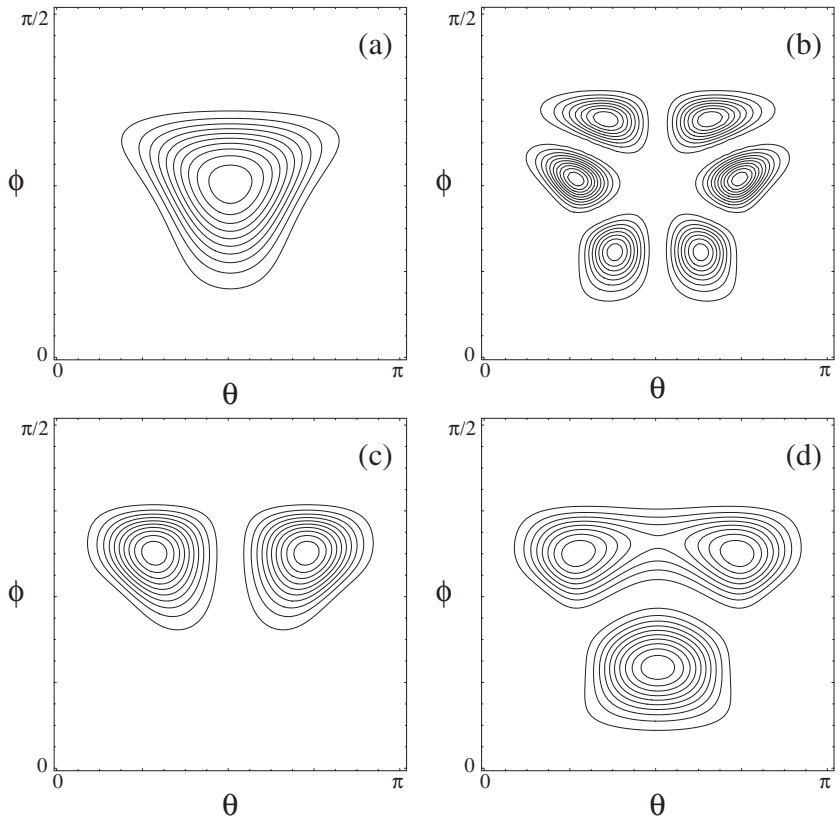

Figure 4. Contour plots of the square of selected rotational component wavefunctions including the volume element $\sin\theta$. At $R = 10.2$ au, (*a*) $I = 0$ for 0^+, and at $R = 12$ au, (*b*) $I = 1$ for 1^+, (*c*) $I = 1$ for 2^+ and (*d*) $I = 1$ for 1^-.

a higher kinetic energy, the low-lying states are occupied by those states that have the fewest nodal lines. Even with our choice of body-frame quantization axis, we can still see this effect in the rotational component wavefunctions, implying that the choice of quantization axis is not essential. The weights of each body-frame component would certainly change, but the number of nodal surfaces would remain the same.

In figure 4 we show some examples of the square of the rotational component wavefunction on the (ϕ, θ) plane calculated at the R values indicated. In figure 4(*a*) for $J = 0$, the density has no nodal lines and peaks at the equilateral triangle geometry near $\theta = \pi/2$ and $\phi = 0.734$. Figure 4(*b*) for 1^+ ($I = 1$—the $I = 0$ component is identically zero since $P = -1$) shows that this state has three nodal lines in agreement with the analysis of Bao *et al* [11]. Because there are three nodal lines, the potential curve for 1^+ is very repulsive, as seen in figure 1. In the two cases above, each wavefunction has only one rotational component, and thus the contour plots also represent the density distributions of the three particles.

We next consider 2^+ and 1^-, which have three and two rotational components, respectively. For 2^+, the $I = 2$ component is nodeless like the 0^+ state in figure 4(*a*). The $I = 1$ component has a node, as shown in figure 4(*c*). The $I = 0$ component also has no node but is distributed differently, with the maximum away from the equilateral triangle configuration. The weights for the three components are given in table 1, showing the predominance of the $I = 0$ and 2

Table 1. Weights of the I-components of $^4He_3$. The $J = 0$ weight is calculated at $R = 10.2$ au while the rest are calculated at $R = 12$ au.

J^π	$I = 0$	$I = 1$	$I = 2$	$I = 3$
0^+	1.0			
1^+		1.0		
1^-	0.302	0.698		
2^+	0.478	0.159	0.363	
2^-		0.730	0.270	
3^+		0.309	0.503	0.188
3^-	0.228	0.646	0.073	0.053

components for 2^+. For 1^-, the $I = 0$ component is similar to figure 4(c) with a nodal line at $\theta = \pi/2$. The $I = 1$ component is shown in figure 4(d). It has a nodal line at a nearly constant ϕ. The fact that there are rotational components that have no nodal lines for 2^+ means that the 2^+ curve is lower in energy. For 1^-, both components have one nodal line, and thus its potential curve is higher.

Similar analysis shows that the $I = 1$ and 3 components of 3^- have no nodes, while the $I = 0$ and 2 components each have a nodal line along $\theta = \pi/2$, and the weight is largest for the $I = 1$ component (see table 1). For 2^-, the $I = 1$ component is similar to figure 4(d), and the $I = 2$ component is similar to figure 4(c). Both components have one node, and thus the potential curve is higher. For 3^+, all three rotational component wavefunctions have one nodal line, and the 3^+ curve is very repulsive.

The origin of the nodal line at $\theta = \pi/2$ in figures 4(b) and (c) and the two additional nodal lines in figure 4(b) emerges more clearly as permutational symmetry requirements when the analysis of Bao *et al* [11] is adopted. Since these nodal lines are the consequence of quantum statistics, their locations are independent of the hyper-radius R. Therefore, this analysis shows that quantum statistics imposes severe constraints on the rotational component wavefunctions that are reflected in the ordering of the potential curves. A similar analysis has been used to investigate the relative positions of the energy levels of triply excited states of atoms [20].

In summary, we have calculated the adiabatic hyperspherical potential curves for the nonzero angular momentum states for $^4He_3$ and $^4He_2{}^3He$. From the repulsive nature of these curves, we conclude that there are no $J \neq 0$ bound states for either system, ruling out the possibility of finding any bound states for nonzero angular momenta in $^4He_3$. The adiabatic hyperspherical approximation is a powerful method for searching for the existence of diffuse bound states since the binding energy need not be directly calculated. Rather, their existence can often be inferred directly from the calculated potential curves. For $^4He_3$, for example, the curves have no attractive well for $J > 0$, while for $^4He_2{}^3He$ a direct solution of the hyper-radial equation for 1^- shows that there are no bound states.

This work is supported in part by the Division of Chemical Sciences, Office of Basic Energy Sciences, Office of Science, US Department of Energy. The authors acknowledge useful conversations with E Nielsen in the early stages of this work, and CDL acknowledges helpful correspondence with Dr C G Bao.

References

[1] Esry B D, Lin C D and Greene C H 1996 *Phys. Rev.* A **54** 394
[2] Blume D and Greene C H 2000 *J. Chem. Phys.* **112** 8052
[3] Nielsen E, Fedorov D V and Jensen A S 1998 *J. Phys. B: At. Mol. Opt. Phys.* **31** 4085

[4] Lewerenz M 1997 *J. Chem. Phys.* **106** 4596
[5] González-Lezana T, Rubayo-Soneira J, Miret-Artés S, Gianturco F A, Delgado-Barrio G and Villarreal P 1999 *Phys. Rev. Lett.* **82** 1648
González-Lezana T, Rubayo-Soneira J, Miret-Artés S, Gianturco F A, Delgado-Barrio G and Villarreal P 1999 *J. Chem. Phys.* **110** 9000
[6] Bruch L W 1999 *J. Chem. Phys.* **110** 2410
[7] Luo F, McBane G C, Kim G, Giese C F and Gentry W R 1993 *J. Chem. Phys.* **98** 3564
[8] Schöllkopf W and Toennies J P 1994 *Science* **226** 1345
[9] Schöllkopf W and Toennies J P 1996 *J. Chem. Phys.* **104** 1155
[10] Luo F, Giese C F and Gentry W R 1996 *J. Chem. Phys.* **104** 1151
[11] Bao C G, Xie W F and Ruan W Y 1997 *Few-Body Syst.* **22** 135
[12] Zhou Y and Lin C D 1994 *J. Phys. B: At. Mol. Opt. Phys.* **27** 5065
[13] Aziz R A and Slaman M J 1991 *J. Chem. Phys.* **94** 8047
[14] Whitten R C and Smith F T 1968 *J. Math. Phys.* **9** 1103
[15] Nielsen E 1999 *PhD Thesis* Aarhus University
[16] Bhatia A K and Temkin A 1964 *Rev. Mod. Phys.* **36** 1050
[17] Sucre M G, Goychman F and Lefebvre R 1970 *Phys. Rev.* A **2** 1738
[18] Roeggen I and Almlöf J 1995 *J. Chem. Phys.* **102** 7095
[19] Aziz R A, Janzen A R and Moldover M R 1995 *Phys. Rev. Lett.* **74** 1586
[20] Morishita T and Lin C D 1998 *Phys. Rev.* A **57** 4268